McAuliffe of the Manchester Institute of Science and Technology for performing the elemental analysis on tetrazene **10**. Financial support by the donors of the Petroleum Research Fund, administered by the American Chemical Society, is gratefully acknowledged.

## References and Notes

(1) H. Zollinger, "Diazo and Azo Chemistry", Interscience, New York, 1961, p 146.
(2) K. Clusius and H. Craubner, *Helv. Chim. Acta*, **38**, 1060 (1955).
(3) B. T. NewBold, "The Chemistry of the Hydrazo, Azo and Azoxy Groups", S. Patal, Ed., Wiley, New York, 1975, p 564.
(4) C. Rüchardt, E. Merz, B. Freudenberg, H. J. Opgenorth, C. C. Tan, and R. Werner, "Essays on Free-Radical Chemistry", *Chem. Soc., Spec. Publ.*, **No. 24**, 51 (1970).
(5) R. G. Lawler and H. R. Ward, *Acc. Chem. Res.*, **5**, 18 (1972).
(6) (a) A. Rieker, P. Niederer, and D. Leibfritz, *Tetrahedron Lett.*, 4287 (1969); (b) S. Berger, S. Hauff, P. Niederer, and A. Rieker, *Ibid.*, 2581 (1972); (c) N. N. Bubnov, K. A. Bilevitch, L. A. Poljakova, and O. Y. Okhlobystin, *J. Chem. Soc., Chem. Commun.*, 1058 (1972); (d) E. Lippmaa, T. Pehk, and T. Saluvere, *Ind. Chim. Belge*, 1070 (1971); (e) A. Rieker, *Ibid.*, 1078 (1971); (f) W. T. Evanochko and P. B. Shevlin, *J. Am. Chem. Soc.*, **100**, 6428 (1978).
(7) J. Q. Adams and J. R. Thomas, *J. Chem. Phys.*, **39**, 1904 (1963).
(8) R. Kaptein, *Chem. Commun.*, 732 (1971).
(9) D. Petredis, A. Burke, and A. L. Balch, *J. Am. Chem. Soc.*, **92**, 428 (1970).
(10) S. Mannen and H. A. Itano, *Tetrahedron*, **29**, 3497 (1973).
(11) (a) I. P. Gragerov, L. A. Kiprianova, A. F. Levit, and T. G. Sterlyova, *Tetrahedron Lett.*, 859 (1976); (b) T. G. Sterlyova, L. A. Kiprianova, A. F. Levit, and I. P. Gragerov, *Zh. Org. Khim.*, **12**, 406 (1976).
(12) Although the reduction potentials of these hydrazyl radicals have not been reported, it is expected that they will parallel those of the corresponding hydrazines. It has been reported[13] that the reduction potential of phenylhydrazine is less than that of *p*-nitrophenylhydrazine by 0.02 V.
(13) Y. Nagata, I. Tachi, and K. Kitao, *Collect. Czech. Chem. Commun.*, **25**, 3271 (1960).
(14) Tetrazene intermediates have been observed at low temperatures in the reaction of diazonium ions with heterocyclic hydrazines.[15]
(15) L. Dežman, D. Janežič, M. Kokalj, E. Kozak, J. Primc, B. Stanovnik, M. Tišler, and O. Zaplotnik-Naglič, *Tetrahedron*, **33**, 2851 (1977).
(16) A. I. Vogel, "A Textbook of Practical Organic Chemistry", 3rd ed., Longman, London, 1957, p 590 ff.

# Substituent Effects on the General- and Specific-Acid-Catalyzed Hydrolyses of Acetals of Benzaldehydes[1]

**James L. Jensen,* Larry R. Herold, Paul A. Lenz, Sevim Trusty, Vincent Sergi, Kenneth Bell, and Patricia Rogers**

*Contribution from the Chemistry Department, California State University, Long Beach, California 90840.* *Received August 13, 1978*

**Abstract:** The effects of solvent and substituents on the general-acid-catalyzed (GAC) hydrolysis of acetals of benzaldehydes are defined. Contrary to earlier reports, GAC hydrolysis is important for a broad spectrum of benzaldehyde acetals. A variety of linear free energy relationship (LFER) cross correlations are established so that the Brønsted $\alpha$ may be calculated for nearly any acetal of any benzaldehyde. The smallest $\alpha$ measured is 0.70 for the hydrolysis of benzaldehyde trifluoroethyl ethyl acetal and the largest is defined as >0.9 for the hydrolysis of *m*-chlorobenzaldehyde diethyl acetal. Procedures for accurately measuring large $\alpha$ values are established. These results reemphasize the importance of defining $\alpha$ as opposed to use of the more ambiguous term specific acid catalysis. The mechanistic implications of LFER cross correlations are discussed in terms of Jencks–O'Ferrall diagrams. Evidence is summarized for rate-determining diffusional separation of the (carboxonium ion)·(conjugate base of the catalyzing acid)·(alcohol) aggregate.

The hydrolysis of acetals has received wide attention in recent years, culminating in two recent review articles.[2] Consensus of opinion appears to be that acetals hydrolyze by an Al mechanism (eq 1) except in certain "special" cases.[2,3]

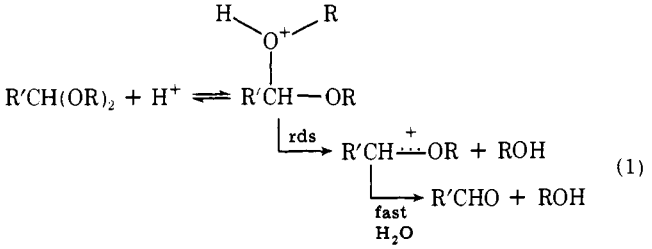


(1)

In previous communications it has been shown that, for R′ = Ar, hemiacetals build up in solution to sizable concentrations (ca. 40% of the total substrate concentration, in some cases);[4] in this paper attention is focused on the chemistry occurring during the initial carboxonium ion forming portion of the reaction, as indicated by eq 1. In particular, data are presented to show that when R′ = Ar and R = alkyl, the first two steps of eq 1 are merged and hydrolysis occurs by a "concerted catalysis" pathway.[5] Indeed, it now appears that acetals and ketals hydrolyze in aqueous solution by this common pathway, although the rate-determining step may differ, depending on the nature of R′ and R. This work supports the suggestion that diffusional separation of the (carboxonium ion)·(conjugate base of the acid catalyst)·(alcohol) aggregate may be rate determining[6,7] and suggests a proper function for Asp 52 in the active site of lysozyme.

## Experimental Section

**Materials.** Reagent grade dioxane was refluxed over $LiAlH_4$ or sodium metal for several hours, distilled, and stored in brown bottles in the freezer until used. The variously substituted benzaldehydes, ethyl orthoformate, propargyl alcohol (propynol), 2,2,2-trifluoroethanol, 2-chloroethanol, and 2-methoxyethanol were the best grade available from Aldrich Chemical Co.

Diethyl acetals of benzaldehydes were synthesized by traditional methods. Diethyl and dimethyl acetals were conveniently prepared from the appropriate benzaldehyde, ethyl or methyl orthoformate, and a catalytic amount of toluenesulfonic acid.[8] Other dialkyl acetals (e.g., di-2-chloroethyl acetals) were conveniently prepared from the appropriate benzaldehyde, alcohol (e.g., 2-chloroethanol), and a catalytic amount of toluenesulfonic acid in benzene (the water formed as the reaction proceeds was removed azeotropically using a Dean-Stark trap).[9]

0002-7863/79/1501-4672$01.00/0 

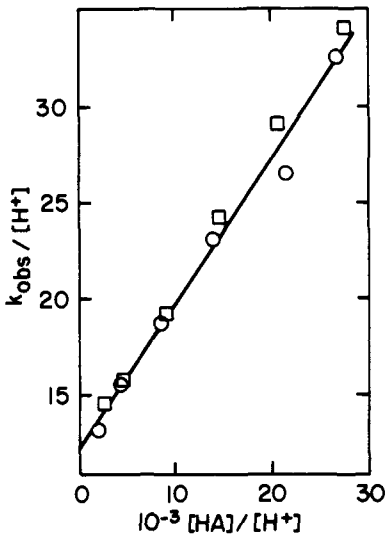


**Figure 1.** A plot showing the dependence of $k_{obsd}$ on the acetic acid concentration for the hydrolysis of benzaldehyde *O*-ethyl *O*-trifluoroethyl acetal at 25 °C and $\mu$ = 0.5 (KCl). $k_{obsd}/[H^+]$ is plotted vs. [HOAc]/[H⁺] (cf. eq 2 discussion); ○ points are at pH 4.65 (±0.05), [HOAc]/[OAc] = 1.0 and □ points are at pH 4.98 (±0.06), [HOAc]/[OAc] = 0.50. The slope = $k_{ac}$ = 7.84 × $10^{-4}$ $M^{-1}$ $s^{-1}$, the intercept = $k_{H^+}$ = 12.3 $M^{-1}$ $s^{-1}$, and the correlation coefficient is 0.996.

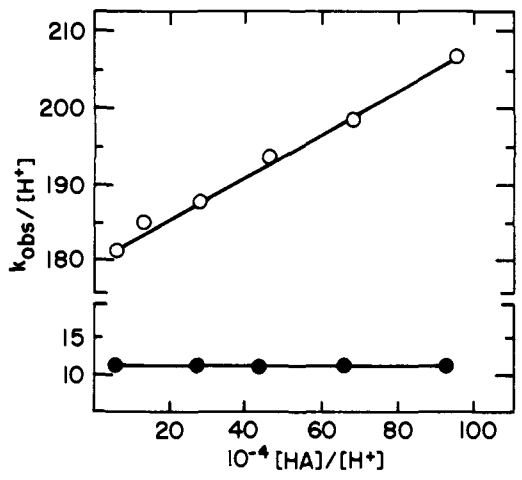


**Figure 2.** A same-scale superimposition of Figure 1-type plots for the hydrolyses of diethyl acetals of benzaldehyde (○, slope = $k_{cac}$ = 3.01 × $10^{-5}$ $M^{-1}$ $s^{-1}$, intercept = $k_{H^+}$ = 180 $M^{-1}$ $s^{-1}$, corr = 0.996) and *m*-chlorobenzaldehyde (●, slope = $k_{cac}$ = 0, intercept = $k_{H^+}$ = 12 $M^{-1}$ $s^{-1}$) in cacodylic acid buffers, $\mu$ = 0.5 (KCl), 25 °C, [HA]/[A⁻] = 2.0, [cacodylic acid] varied from 0.08 to 0.80 M.

Mixed acetals, e.g., benzaldehyde *O*-ethyl *O*-2-chloroethyl acetal, were prepared by an adaptation of analogous literature procedures.[3b,10] Typically, 0.6 mol of the diethyl acetal of benzaldehyde was mixed with 0.6 mol of thionyl chloride. After standing for 30 min, the volatile side products and excess thionyl chloride were removed by vacuum distillation at 30 Torr to a pot temperature of 100 °C. Vacuum distillation at ca. 1 Torr produced an essentially quantitative yield of the $\alpha$-chloro ether, $\alpha$-chloro-$\alpha$-ethoxytoluene (bp 72–74 °C, 1 mm). Because of the high reactivity and toxicity of $\alpha$-chloro ethers, the distillate was collected in 0.1-mol batches in round-bottomed flasks containing 0.1 mol of the appropriate alcohol, 0.11 mol of NaH, and 100 mL of DMF. A special fraction cutter was used which allowed the addition of the $\alpha$-chloro ether to the stirred DMF solution to be made at room pressure without interrupting the vacuum distillation. Following a basic aqueous workup procedure, 50–75% yields of vacuum-distilled *O*-ethyl *O*-alkyl acetals were obtained and ascertained to be pure by $^1$H NMR analysis.

**Kinetic Method.** Reactions were monitored at the absorption maximum of the benzaldehyde produced by hydrolysis, using either a Beckman Kintrac VII or a Beckman Recording DU with a specially constructed constant-temperature bath positioned between the monochromator and the phototube housing. (In the latter case the temperature was maintained at 25.00 ± 0.02 °C.)[11] Reaction conditions were pseudo first order and plots of log $(A_\infty - A_t)$ against time were linear for at least 3 half-lives of reaction time. Rate constants were calculated from these graphs and also by a computer program which fitted data for the first 3 half-lives to the best first-order curve of absorbance vs. time, using $A_\infty$ as a variable.[12] Typically, the $A_\infty$ values calculated by the computer program agreed with the experimentally observed values, except for some of the very slow reactions where it was inconvenient to wait for the absorbance to reach $A_\infty$ (particularly in phosphate buffers, where the experimental $A_\infty$ decreased with time, associated with the observed growth of organisms in the cuvette solution).

Second-order rate constants were calculated from the observed rate constants according to

$$k_{obsd} = k_{H^+}[H^+] + k_{HA}[HA] \qquad (2)$$

where ([H⁺] is antilog (−pH), as measured by a Beckman Model 4500 pH meter using a combination glass electrode. In most cases it was possible to measure $k_{H^+}$ in $10^{-3}$–$10^{-1}$ N HCl solutions where the last term of eq 2 is negligible. For buffer solutions, plots of $k_{obsd}/[H^+]$ against [HA]/[H⁺] produced straight lines (cf. Figure 1) whose slope = $k_{HA}$ and intercept = $k_{H^+}$. (In no cases were pH-independent terms detectable in eq 2.) Values of $k_{H^+}$ obtained from the intercept were identical with those obtained in dilute HCl solutions. Slopes of plots such as Figure 1 were independent of buffer ratio. The advantage of plotting $k_{obsd}/[H^+]$ against [HA]/[H⁺] is that *it* takes into account the slight dependence of pH on the buffer concentration which arises because of the small specific salt effect on $pK_{HA}$. Values of $pK_{HA}$ which are cited are values at zero buffer concentration and 0.5 N KCl (obtained by extrapolation of a plot of $pK_{HA}$ against [buffer] to [buffer] = 0).

## Results

**Hemiacetal Buildup.** Most of the kinetic studies in buffers were at a sufficiently high pH to ensure that the hemiacetal hydrolyzed quickly to benzaldehyde via a base-catalyzed pathway, thus assuring that the rate-determining step was truly acetal hydrolysis and not hemiacetal hydrolysis.[4a] In dilute HCl solution, the first 10–20% reaction was not first order because of the time required to produce a pseudo-steady-state amount of hemiacetal; however, the absorbance-time data exhibited first-order behavior throughout the rest of the measurable reaction and it has been shown that the rate measured for this portion of the reaction is essentially that of acetal hydrolysis.[4a]

**General Acid Catalysis.** Plots such as Figure 1 show that acetals of benzaldehydes hydrolyze by a process that exhibits a rate dependence on buffer concentration. These rates can be analyzed according to eq 2 as described; however, two concerns remain.

(1) It must be demonstrated that it is the acid component of the buffer which functions as catalyst. This can be unambiguously demonstrated by showing that the slopes of plots such as Figure 1 are independent of buffer ratio; such was the case in all our experiments (cf. Figure 2).

(2) For cases where the slopes of plots such as Figure 1 are shallow, there must be some assurance that "catalysis" is not merely a specific salt effect.[13] One of the least ambiguous "checks" is that used in this study. A reaction may be shown to exhibit a rate dependence on buffer concentration well above that for some closely related reaction. That is, the closely related reaction can be used to "calibrate" the specific salt effect. For those cases where no rate dependence on [buffer] existed (e.g., substrates with large $\alpha$ studied in the more acidic buffers), plots such as Figure 1 had a slope of zero. Thus, there appears to be no detectable specific salt effect in aqueous buffer solutions. This point is not trivial and was not easily resolved. For example, a portion of this study was intended to investigate the effects of mixed solvents on general acid catalysis; however, even in 20% dioxane-water or 20% $Me_2SO$-water mixtures,

**Table I.** Second-Order Rate Constants for the General-Acid-Catalyzed Hydrolyses of Dialkyl Acetals of Para-Substituted Benzaldehydes in Water at 25 °C, $\mu$ = 0.5 (KCl)[a]

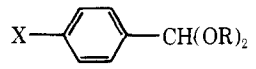

| OR | $10^5k_{mp}$[b] | $10^4k_p$[c] | $10^4k_{mes}$[d] | $10^4k_{cac}$[e] | $10^3k_{ac}$[f] | $10^2k_F$[g] | $k_{H^+}$ | $\alpha$[h] | corr[i] |
|---|---|---|---|---|---|---|---|---|---|
| | | | | X = $Me_2N$ | | | | | |
| $OCH_2CH_3$ | 308 | 88.5 | | 251 | | | 30,400 | 0.81 | 0.999 96 |
| | | | | X = $CH_3O$ | | | | | |
| $OCH_2CH_3$ | 11.4 | | 5.83 | 7.64 | | | 2 450 | 0.85 | 0.999 90 |
| $OCH_2CH_2OCH_3$ | | | 0.681 | 1.56 | 3.10 | | 262 | 0.83 | 0.999 90 |
| $OCH_2CH_2Cl$ | 0.743 | 0.367 | | 0.942 | 1.02 | 1.12 | 61.8 | 0.78 | 0.9990 |
| | | | | X = $CH_3$ | | | | | |
| $OCH_2CH_3$ | | | 1.33 | 2.19 | | | 725 | 0.86 | 0.999 991 |
| | | | | X = H | | | | | |
| $OCH_2CH_3$ | | | 0.307 | 2.95 | 0.858 | | 169 | 0.87 | 0.9994 |
| $OCH_2CH_2OCH_3$ | | | | 0.0359 | 0.079 | | 16.8 | 0.88 | 0.999 95 |
| $OCH_2CH_2Cl$ | | | | | 0.0362 | | 3.98 | 0.84 | |
| $pK'_{HA}$[j] | 7.41 | 6.59 | 6.18 | 6.19 | 4.59 | 3.53 | | | |

[a] Mean values of replicate determinations at different buffer ratios; the standard deviation typically is ±2–5% for $k_{H^+}$ and ±5–10% for $k_{HA}$ values. [b] mp = $CH_3PO_3H^-$. [c] p = $H_2PO_4^-$. [d] mes = 2-(*N*-morpholino)ethanesulfonic acid, a Calbiochem buffer. [e] cac = $(CH_3)_2AsO_2H$. [f] ac = $CH_3CO_2H$. [g] F = $HCO_2H$. [h] $\alpha$ = Brønsted $\alpha$. [i] corr = correlation coefficient. [j] $pK'_{HA}$ = $pK_a$ of the buffer acid HA at $\mu$ = 0.5 and zero buffer concentration.

**Table II.** Second-Order Rate Constants for the General-Acid-Catalyzed Hydrolyses of Benzaldehyde *O*-Ethyl *O*-Alkyl Acetals in Water at 25 °C, $\mu$ = 0.5 (KCl)[a]

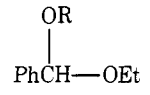

| OR | $10^5k_{mes}$[b] | $10^5k_{cac}$[c] | $10^4k_{ac}$[d] | $10^3k_F$[e] | $k_{H^+}$[h] | $\alpha$[f] | corr[g] |
|---|---|---|---|---|---|---|---|
| $OCH_2CH_3$ | 3.07 | 2.95 | 8.58 | | 169 | 0.87 | 0.9994 |
| $OCH_3$ | 1.18 | 1.80 | 5.80 | | 122 | 0.89 | 0.999 94 |
| $OCH_2CH_2OCH_3$ | | 2.81 | 5.26 | 8.52 | 82.6 | 0.86 | 0.991 |
| $OCH_2CH_2Cl$ | | 2.48 | 5.02 | 3.54 | 50.5 | 0.83 | 0.999 95 |
| $OCH_2C{\equiv}CH$ | | 3.97 | 5.86 | 6.60 | 37.3 | 0.79 | 0.9994 |
| $OCH_2CF_3$ | | 6.78 | 7.82 | 4.47 | 12.6 | 0.70 | 0.999 95 |

[a] Mean values of replicate determinations at different buffer ratios; the standard deviation typically is ±2–5% for $k_{H^+}$ and ±5–10% for $k_{HA}$ values. [b] mes = 2-(*N*-morpholino)ethanesulfonic acid (a Calbiochem buffer). [c] cac = $(CH_3)_2AsO_2H$. [d] ac = $CH_3CO_2H$. [e] F = $HCO_2H$. [f] $\alpha$ = Brønsted $\alpha$. [g] corr = correlation coefficient. [h] $\rho^*$ = −1.06 (corr = 0.992).

a significant negative salt effect was observed. (Plots such as Figure 2 for mixed solvent systems produced a line of significant negative slope for the hydrolysis of *m*-chlorobenzaldehyde diethyl acetal). Such behavior was eliminated by the use of KCl as the common salt and by the use of a totally aqueous solvent. The decision to work at $\mu$ = 0.5 was dictated by the marginal solubility of some of the acetals at higher ionic strengths.

The substance showing the largest $\alpha$ (the least general acid catalysis) is the diethyl acetal of benzaldehyde. Figure 2 displays a comparison of the rate dependence on buffer concentration for the diethyl acetals of benzaldehyde and *m*-chlorobenzaldehyde. The slopes of the lines for the two substances are significantly different and the difference in slope is dependent upon the buffer acid; however, in both cacodylic acid and acetic acid buffers the slope of the line for *m*-chlorobenzaldehyde diethyl acetal is essentially zero. Therefore, we are confident that the $k_{HA}$ calculated for benzaldehyde diethyl acetal from the slopes of plots such as Figure 2 is truly the rate constant for that portion of the hydrolysis catalyzed by the buffer acid as defined by eq 2.

The Brønsted plots constructed from the data of Tables I and II show no detectable dependence of $k_{HA}$ on charge type; i.e., the points for buffers of the type $RPO_3H^-$ and the zwitterionic MES buffer lie on the line established by the proton and $RCO_2H$ points. Thus the type of charge effect reported by Kresge[21] for the general-acid-catalyzed hydrolyses of vinyl ethers is not significant for the hydrolyses of acetals of benzaldehydes.

## Discussion

**General Acid Catalysis.** The observation of general acid catalysis for the variety of acetals of benzaldehydes listed in Tables I and II requires that eq 1 be incorrect for these hydrolyses. The mechanism formerly proposed[2,3] for the "special cases" is eq 3.

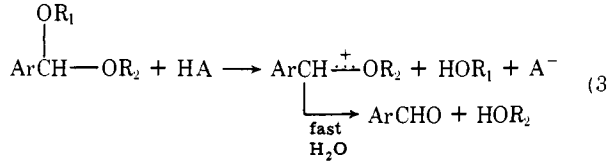

(3)

It is instructive to consider this mechanism for the present series because it affords the first opportunity to observe the transition from a "special case" acetal (where general acid catalysis is observed) to a "typical" acetal (where general acid catalysis is not observed). It is particularly informative to analyze this system using the Jencks-O'Ferrall approach[5,14] as described by Figure 3. Taking the diethyl acetal of benzaldehyde as the reference compound, the large Brønsted $\alpha$ (0.87,

**Table III.** Second-Order Rate Constants for the Hydrolyses of Diethyl Acetals of Substituted Benzaldehydes in Water and Dioxane–Water Mixtures at 25 °C, $\mu$ = 0.5 (KCl)

| | $k_{H^+}$[a] | | |
|---|---|---|---|
| substituent | water | 20% dioxane–water | 50% dioxane–water |
| *p*-$NO_2$ | 0.519 | 0.221 | 0.287 |
| *m*-$NO_2$ | 0.952 | 0.393 | 0.0402 |
| *m*-Cl | 11.5 | 5.03 | 0.466 |
| *m*-$OCH_3$ | 82.8 | 43.7 | 8.15 |
| H | 169 | 94.2 | 15.8 |
| *m*-$CH_3$ | 233 | 142 | 22.7 |
| *p*-$CH_3$ | 725 | 415 | 81.7 |
| *p*-$OCH_3$ | 2 450 | 1 580 | 491 |
| *p*-$NMe_2$ | 30 400 | 44 700 | 21 100 |
| $\rho$[b] | −3.16 (0.999) | −3.35 (0.999) | −3.58 (0.996) |
| $\rho_r$[b] | −0.29 | −0.60 | −0.93 |

[a] $k_{H^+} = k_{obsd}/[H^+]$. Values listed are means of replicate measurements. $k_{H^+}$ is independent of pH′. Average deviations from the means of replicate determinations of $k_{H^+}$ were <±5%. [b] Calculated after the method of ref 6. Values in parentheses are correlation coefficients for the line generated by meta and electron-withdrawing substituents. $\sigma$ values taken from J. Hine, "Structural Effects on Equilibria in Organic Chemistry", Wiley, New York, 1975.

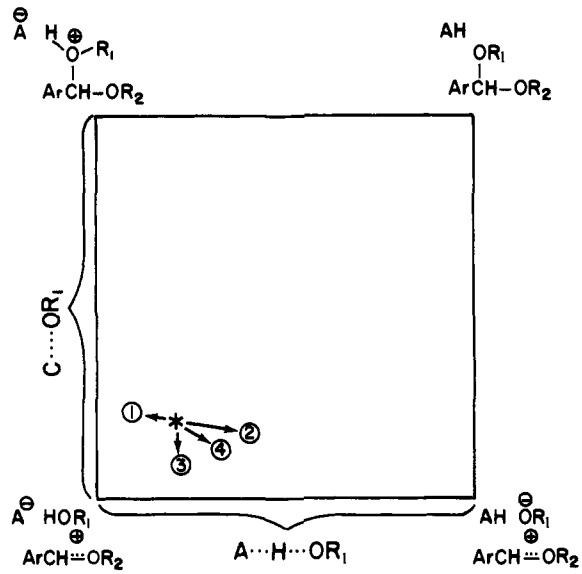


**Figure 3.** A Jencks–O'Farrell diagram for the hydrolysis of acetals of benzaldehydes according to eq 3. The location of the transition state for the proton-catalyzed hydrolysis of benzaldehyde diethyl acetal is located by an asterisk. The transition-state motion imparted by electron-withdrawing groups in the Ar and $R_2$ moieties is shown by ①, that of electron-donating groups in Ar and $R_2$ by ②, that of weaker catalyzing acids HA by ③, and that of electron-withdrawing groups in $R_1$ by ④.

Table I) and Hammett $\rho$ (−3.2, Table III) locate the transition state in the lower left quadrant as shown. The following observations are derived from the $\alpha$ and $\rho$ values in Tables I–III.

(a) Electron-donating groups in the Ar moiety lower the entire bottom side of the diagram in Figure 3, which causes a Hammond motion along the reaction coordinate and movement orthogonal to the reaction coordinate which sum to move the transition state in the direction designated by ② in Figure 3. This conceptual argument is corroborated by the $\alpha$ values of 0.87, 0.86, and 0.81 for the diethyl acetals of benzaldehyde, *p*-methyl-, *p*-methoxy-, and *p*-dimethylaminobenzaldehyde. Note that the effect of electron-withdrawing groups in the Ar moiety is just the opposite, as indicated by the motion designated ①. This is consistent with our observation that the diethyl acetal of *m*-chlorobenzaldehyde did not exhibit catalysis in the same buffers as did the diethyl acetal of benzaldehyde (i.e., $\alpha$ for the former must be greater than $\alpha$ for the latter). From the data in Table I, $\partial\alpha/\partial\sigma = 0.073$ (correlation coefficient = 0.999), which simply quantitates the observation that $\alpha$ is only slightly sensitive to the extent of electron donation from the aryl moiety. From this Cordes-type relationship,[15] $\alpha$ for the diethyl acetal of *m*-chlorobenzaldehyde may be calculated to be 0.90; this is consistent with our lack of observing even a 10% rate enhancement in 1 M cacodylic acid buffers, which requires $\alpha \geq 0.91$.[16]

(b) As the catalyzing acid HA becomes weaker, the entire left side rises, causing Hammond motion along the reaction coordinate and movement orthogonal to the reaction coordinate which sum to move the transition state in the general direction designated by ③ in Figure 3. This is corroborated by the observation that $\alpha$ decreases with $\sigma$, which is equivalent to saying that $\rho$ decreases as $pK_{HA}$ increases. Lack of much horizontal motion in ③ is consistent with the observation that the $k_{H^+}$ point lies on the line of the Brønsted plot. As will be elaborated further in another context, it is interesting to note that $(\partial\rho/\partial pK_{HA}) \neq 0$ requires that at some point a reversal of substituent effect occur; i.e., $\rho$ must become positive when the catalyzing acid is sufficiently weak. In the present case, $pK_{HA}$ would have to be impossibly large to observe this reversal of sign (larger than $pK_{H_2O}$), but this is simply a result of a large negative $\rho$ for $k_{H^+}$ and a rather small $\partial\rho/\partial pK_{HA}$.

(c) As $R_1$ becomes electron withdrawing (relative to ethyl), the upper left corner rises and the lower right corner lowers, resulting in a marked movement of the transition state in a direction orthogonal to the reaction coordinate, as designated by ④. This is corroborated by the marked decrease in $\alpha$ shown in Table II, $\alpha = 0.87$ for $R_1 = CH_2CH_3$ through $\alpha = 0.70$ for $R_1 = CH_2CF_3$. We have no evidence supporting the vertical motion shown by ④; the extent of this motion depends upon the direction of the reaction coordinate—we believe most of the motion shown by ④ to be horizontal rather than vertical because the reaction coordinate is probably biased toward the upper left corner for $R_1 = CH_2CH_3$. The $\partial\alpha/\partial\sigma^*$ correlation for this series is nonlinear, as shown in Figure 4. There are two possible explanations for the decreasing slope in moving from $R_1 = CH_2CF_3$ to $R_1 = CH_2CH_3$ on the plot of $\alpha$ vs. $\sigma^*$. First, it may be that a large energy barrier exists as the lower side of Figure 3 is approached, resulting in a "leveling off" of the $\partial\alpha/\partial\sigma^*$ curve. The nature of such a barrier should be a function of carboxonium ion stability; i.e., it should be affected by the shape/depth of the potential energy well in the lower left corner. The second explanation is that the "leveling off" is caused by a change in rate-determining step. An attractive mechanism is given by eq 4. As $R_1$ becomes more electron

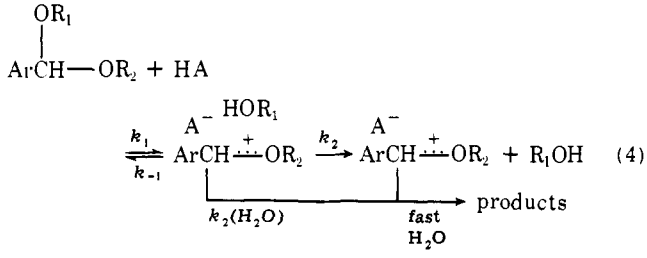


withdrawing, $R_1OH$ becomes much less nucleophilic, which decreases $v_{-1}$ relative to $v_2$; when $v_2 > v_{-1}$, $v_1$ is rate determining (as for $R_1 = CH_2CF_3$); when $v_{-1} > v_2$, $v_2$ is rate determining (as for $R_1 = CH_2CH_3$). The presence of the conjugate base of the catalyzing acid in the transition state for the rate-limiting diffusional separation process is responsible for the slight catalysis observed ($\alpha \simeq 0.88$). In the reverse direction, this amounts to a "preassociation" general-base-catalyzed mechanism.[17]

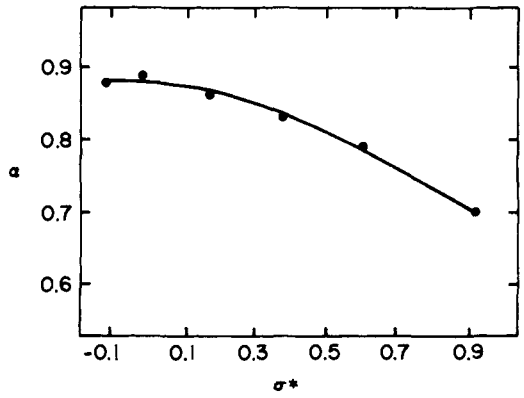


Figure 4. A plot of the Brønsted $\alpha$ vs. $\sigma^*$ for the general-acid-catalyzed hydrolysis of benzaldehyde *O*-ethyl *O*-alkyl acetals.

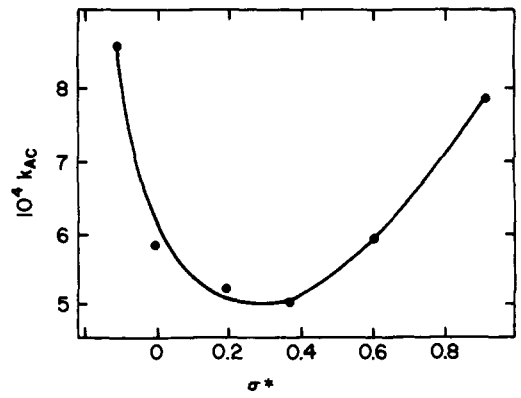


Figure 5. A plot of $k_{ac}$ vs. $\sigma^*$ for the acetic acid catalyzed hydrolysis of benzaldehyde *O*-ethyl *O*-alkyl acetals.

At the present time we have no evidence regarding the role of water in eq 4; it is possible that, as the carboxonium ion becomes more reactive and/or $R_1OH$ becomes more nucleophilic, the rate-determining step involves nucleophilic attack by the water. (We are beginning solvent and secondary isotope effect studies to answer this point.) For the sake of the present discussion, no distinction is made between $k_2$ and $k_2(H_2O)$; both are lumped together as $k_2$ processes.

Although the alternative explanations just presented are difficult to distinguish experimentally, several observations suggest that $k_2$ processes may be rate determining in some instances. Values of $k_{H^+}$ for the series in Table II vary by only 15-fold while $\alpha$ changes from 0.70 to 0.87, whereas for the diethyl acetals of substituted benzaldehydes (Table I) values of $k_{H^+}$ vary by 3000 while $\alpha$ changes only from 0.81 to 0.9. With reference to Figure 3, it is not clear why the ① and ② changes have such a much smaller effect on $\alpha$ than ④. Measured by any standard (reactivity, $\sigma$, $\sigma^*$, etc.) this is the case: the *major* effect of ① and ② change is perpendicular to the diagram (the energy coordinate) whereas the major effect of ④ change is along the $A\cdots H\cdots OR_1$ axis (horizontal motion on the diagram). This is most easily understood if the diethyl acetal of benzaldehyde hydrolyzes via rate-controlling diffusional separation, as per eq 4, and the rather subtle change in $\alpha$ which accompanies the 3000-fold change in reactivity on going from the diethyl acetal of benzaldehyde to the diethyl acetal of *p*-dimethylaminobenzaldehyde arises from a gradual change in rate-determining step (as $v_{-1}$ decreases relative to $v_2$ in eq 4). That is, for rate-limiting diffusional separation, $\alpha$ ought to be rather independent of the nature of $R_1$ but somewhat dependent on the nature of Ar and $R_2$ (i.e., on carboxonium ion stability) because of ion pairing forces within the (carboxonium ion)·($A^-$)·($R_1OH$) aggregate. Thus increased carboxonium ion stability produces a large rate increase accompanied by a slight decrease in the Brønsted $\alpha$ *when* diffusional separation is rate determining, whereas decreased nucleophilicity in $R_1OH$ results in a change in rate-determining step from $k_2$ to $k_1$, which produces a significant decrease in the Brønsted $\alpha$.

It bears noting that, if the series $ArCH(OEt)_2$ hydrolyzes increasingly with rate-limiting diffusional separation of the aggregate ($v_2$ in eq 4) as Ar becomes electron withdrawing, then almost certainly the simple alkyl acetals of aliphatic aldehydes and ketones do also; that is, eq 4 may be the "normal" or "typical" mechanism of acetal hydrolysis.

An interesting development arises from a different presentation of the data in Table II, as shown in Figure 5 as a plot of $k_{HA}$ vs. $\sigma^*$ for the series of buffer acids. Note that the curve passes through a minimum and that the position of the minimum shifts toward a larger $\sigma^*$ as $pK_{HA}$ decreases (cf. Table II data). This could be the result of $\partial\alpha/\partial\sigma^*$ or $\partial\rho^*/\partial pK_{HA} \neq 0$ (alluded to earlier), where in this case $\rho^*$ for $k_{H^+}$ is sufficiently small ($\rho^* = -1.07$, correlation coefficient = 0.991) so as to allow the inversion of the substituent effect to be observable for moderately weak acids. In a practical sense, this means that $k_{HA}$ increases as $R_1OH$ becomes a better leaving group if the catalyzing acid is sufficiently weak. This could be a result of ③ and ④ motion in Figure 3, which eventually makes the $R_1O$ moiety partially negative in the transition state *when* $R_1$ contains electron withdrawing groups *and* the catalyzing acid is moderately weak. (It is no coincidence that this describes the natural substrates and active site catalysts for the glucosyl transferases.[18])

Alternatively (and preferably), the minimum in Figure 5 can be viewed as a result of a change in rate-determining step in eq 4: the rate decrease with increasing $\sigma^*$ on the left "leg" of the curve, where $v_2$ is rate determining, reflects a commensurate decrease in $k_1$ and the rate increase with increasing $\sigma^*$ on the right "leg" of the curve, where $v_1$ is rate determining, reflects a commensurate increase in $k_1$. That the left leg is of steeper slope than the right leg is a result of the increase in $k_1$ being much less dependent on $\sigma^*$ than the inverse dependence of $k_1$. This is true because of the location of the transition state in Figure 3 for weak catalyzing acids, ③ and ④, and the steeper right "leg" for $k_{cac}$ compared to $k_{ac}$ confirms this motion. (Aside from the points mentioned earlier, another good reason to prefer the rate-limiting diffusional separation alternative is that for the minimum to arise from a $\partial\rho^*/\partial pK_{HA}$ effect requires $\rho^*$ to *decrease* with increasing $pK_{HA}$: we observe essentially no effect on $\rho^*$ of $pK_{HA}$ *for rate-determining* $v_2$ *processes*. This is best represented by the several data points in Figure 4 showing $\partial\alpha/\partial\sigma^* \simeq 0$, which requires that $\partial\rho^*/\partial pK_{HA} \simeq 0$.)

Finally, a brief analysis of the $ArCH(OR)_2$ series, which combines the variables (a) and (c) above, is presented. In this case $R_1 = R_2$ and as $R_2$ becomes electron withdrawing (relative to ethyl) it destabilizes the carboxonium ion just as does an electron-withdrawing aryl group. The aryl group apparently compensates for this increased electronic demand by increased conjugative stabilization: for $ArCH(OEt)_2$ $\rho = -3.16$ and $\rho^r = -0.29$ and for $ArCH(OCH_2CH_2Cl)_2$[22] $\rho = -3.20$ and $\rho^r = -1.3$. More generally, the data in Table I show that when $R_1 = R_2$ contains electronegative groups the reactivity diminishes and $\alpha$ decreases (which again shows that when the leaving group ($R_1$) is better, the predominant effect is reflected in $\alpha$, consistent with the mechanism of eq 4). For a specific case, the di-2-chloroethyl acetal of benzaldehyde reacts 0.08 times as fast as the mixed acetal, benzaldehyde 2-chloroethyl ethyl acetal ($k_{H^+}$ values), but the $\alpha$ values are indistinguishable.

**Solvent Effects.** As tabulated in Table III, the rate of hydrolysis falls off markedly as the percent dioxane in the

aqueous solvent is increased ($\mu$ = 0.5 with KCl) *and* $\rho$ increases from 3.16 in $H_2O$ to 3.58 in 50% dioxane. Also, the resonance stabilization factor $\rho^r$ (as measured by the two-parameter Yukawa-Tsueno equation)[6] increases from −0.29 in water to −0.93 in 50% dioxane. This is precisely as expected from the mechanism of eq 4; as the dielectric constant of the solvent is lowered and the activity of water decreased (and its ability to stabilize ions by solvation), $v_{-1}$ increases relative to $v_2$ and rate-determining diffusional separation will become more important. Since in water we propose $v_2$ rate limiting for those acetals less reactive than benzaldehyde diethyl acetal, in 50% dioxane $\rho$ likewise ought to reflect a transition state with a fully formed carboxonium ion. (Because of the nature of the two-parameter $\sigma\rho$ treatment, all the $\rho$ values represent the substituent effect on the acetal going to a fully formed carboxonium ion transition state). The increasing $\rho$ and $\rho^r$ as percent dioxane is increased is a result of increasing electronic demand on the substituents, brought about by decreased solvation of the carboxonium ion by the solvent.

**Enzyme Catalysis.** These results provide evidence illuminating two features of the chemistry occurring at the active site of lysozyme.[18] First, Asp-52 is present at the active site in the ionized state: our results provide an important role for Asp-52 which need not show up as a high rate acceleration in model systems. Namely, Asp-52 can behave as $A^-$ in the mechanism of eq 4. This may well slow down the collapse of the aggregate by a $v_{-1}$ process and thus favor the leaving group diffusing away. In the absence of any evidence for a covalently bound intermediate (similar to an acylal), this carboxonium ion stabilization is best viewed as electrostatic stabilization (much as originally proposed by Phillips).[18c] Thus, this work provides experimental corroboration of an earlier hypothesis.

The second insight arises from the discussion of Figure 5 and, simply stated, says that the rate of catalysis by Glu-35 of the hydrolysis of the natural substrate is much greater than predicted from previous physical organic models, since the leaving group substituent effect for such a weak catalyzing acid is actually opposite to that of proton catalysis. In this regard, we now are in the process of quantitating this reversal of substituent effects, having noted that Kankaanpera observed substituent effects similar to Figure 3 for *proton*-catalyzed hydrolysis of the 2-alkoxydihydropyrans and dihydrofurans.[19] With reference to eq 4, if $v_2$ is the rate-determining step, then $k_2/k_{-1} < 1.0$ and, provided that Asp-52 can change the rate-determining step to $v_1$, the rate will increase substantially; just as significantly, Glu-35 can now function as a kinetically more efficient general acid catalyst (cf. motions ③ and ④, Figure 3). Thus our results would predict that the major role of Asp-52 is to change the rate-determining step from diffusional separation ($v_2$ in eq 4) to proton transfer concerted with C-O bond cleavage ($v_1$, in eq 4). This is a vital role since the rate enhancement caused by omitting the $k_2/k_{-1}$ term is augmented by the greater catalysis by Glu-35 on $v_1$. Previous physical organic models have not been able to elucidate these roles because this is the first study reporting such an interplay between $pK_{HA}$ and substituent effects on the leaving group in systems showing a probable change in rate-determining step.

Semiquantitatively, Figure 5 allows an estimation of the rate of a rate-determining $v_1$ process relative to the rate of a rate-determining $v_2$ process for the acetic acid catalyzed hydrolysis of benzaldehyde trifluoroethyl ethyl acetal: assuming $\rho^*$ = −1.7 (the slope "established" by the OEt and $OCH_3$ points in Figure 5) for a rate-determining $v_2$ process and extrapolating to the trifluoroethyl group ($\sigma^*$ = 0.92) produces a factor of 50. That is, if this model is correct, acetic acid functions as a catalyst 50 times more effectively when $v_1$ is rate determining than when $v_2$ is rate determining. This factor will increase as the catalyzing acid $pK_a$ increases and as the substituent effect changeover occurs "earlier". Fife has recently reported a rate enhancement of 100-fold for a rate-determining $v_1$ process.[20]

Work is in progress on a model which better represents lysozyme substrates and hopefully a more quantitative measurement of this type of rate enhancement will be provided by that system.

**Acknowledgment.** Support from the National Science Foundation (CHE77-00482) is gratefully acknowledged. Kathleen Cannon synthesized the phosphonate buffers and Raymond Johnson made some of the preliminary kinetic measurements.

## References and Notes

(1) First presented in Abstracts, Pacific Conference on Chemistry and Spectroscopy, Anaheim, Calif., Oct 12–14, 1977, No. 48 and 74, pp 41, 49.
(2) (a) E. H. Cordes and H. G. Bull, *Chem. Rev.*, **74**, 581 (1974); (b) T. H. Fife, *Acc. Chem. Res.*, **5**, 264 (1972).
(3) (a) C. F. Bernasconi and J. R. Gandler, *J. Am. Chem. Soc.*, **100**, 8117 (1970); (b) B. Capon and K. Nimmo, *J. Chem. Soc., Perkin Trans. 2*, 1113 (1975); (c) B. Capon and M. I. Page, *ibid.*, 522 (1972); (d) A. L. Mori, M. A. Porizio, and L. Schaleger, *J. Am. Chem. Soc.*, **94**, 5034 (1972).
(4) (a) J. L. Jensen and P. A. Lenz, *J. Am. Chem. Soc.*, **100**, 1291 (1978); (b) B. Capon, *Pure Appl. Chem.*, **49**, 1001 (1977).
(5) W. P. Jencks, *Chem. Rev.*, **72**, 705 (1972).
(6) P. R. Young and W. P. Jencks, *J. Am. Chem. Soc.*, **99**, 8238 (1977).
(7) M. M. Kreevoy and R. Eliason, *J. Am. Chem. Soc.*, **100**, 7037 (1978).
(8) N. Robjohn, Ed., "Organic Syntheses", Collect Vol. IV, Wiley, New York, 1963, p 21.
(9) E. L. Horning, Ed., "Organic Syntheses", Collect. Vol. III, Wiley, New York, 1955, p 644.
(10) T. H. Fife and E. Anderson, *J. Am. Chem. Soc.*, **92**, 5464 (1970).
(11) J. L. Jensen and D. J. Carre, *J. Org. Chem.*, **36**, 3180 (1971).
(12) J. L. Jensen and D. J. Carre, *J. Org. Chem.*, **39**, 2103 (1974).
(13) (a) J. L. Hogg and W. P. Jencks, *J. Am. Chem. Soc.*, **98**, 5643 (1976); (b) M. Lahti and A. Kankaanpera, *Acta Chem. Scand.*, **24**, 706 (1970).
(14) R. A. More O'Ferrall, *J. Chem. Soc. B*, 274 (1970).
(15) (a) E. H. Cordes and W. P. Jencks, *J. Am. Chem. Soc.*, **84**, 4319 (1962); (b) D. A. Jencks and W. P. Jencks, *ibid.*, **99**, 7948 (1977); (c) L. H. Funderburk and W. P. Jencks, *ibid.*, **100**, 6708 (1978); (d) L. H. Funderburk, L. Aldwin, and W. P. Jencks, *Ibid.*, **100**, 5444 (1978).
(16) J. L. Jensen and W. P. Jencks, *J. Am. Chem. Soc.*, **101**, 1476 (1979).
(17) M. M. Cox and W. P. Jencks, *J. Am. Chem. Soc.*, **100**, 5956 (1978).
(18) (a) T. Imoto, L. N. Johnson, A. C. T. North, D. C. Philips, and J. A. Rupley in "The Enzymes", Vol. VII, P. D. Boyer, Ed., Academic Press, New York, 1972, p 666; (b) B. M. Dunn and T. C. Vruice, *Adv. Enzymol.*, **37**, 1 (1973); (c) D. C. Phillips, *Sci. Am.*, **215**, 78 (1966).
(19) A. Kankaanpera and K. Miikki, *Suom. Kemistil. B*, 41, 42 (1968).
(20) T. H. Fife and T. J. Przystas, *J. Am. Chem. Soc.*, **99**, 6693 (1977).
(21) W. K. Chwang, R. Eliason, and A. J. Kresge, *J. Am. Chem. Soc.*, **99**, 805 (1977).
(22) In addition to data in Table I, $k_{H^+}$ = 1.12 $M^{-1}$ $s^{-1}$ for *p*-Cl and 0.0153 $M^{-1}$ $s^{-1}$ for *m*-$NO_2$; the correlation coefficient for the two-parameter $\rho$ calculation is 0.997.